

Atom-molecule conversion in a periodically driven spin-boson modelSangyong Yi (이 상용)¹ and Sang Wook Kim (김 상욱)^{2,*}¹*Department of Physics, Pusan National University, Busan 609-735, South Korea*²*Department of Physics Education, Pusan National University, Busan 609-735, South Korea*

(Received 13 July 2015; published 19 January 2016)

We have investigated the dynamics of atom-molecule conversion using a periodically driven spin-boson model both quantum mechanically and semiclassically. The semiclassical dynamics is fully chaotic for small driving frequencies, so that the regular atom-molecule conversion gradually vanishes. In quantum mechanics, however, the periodic conversion takes place at small frequencies since the quantum adiabatic condition is fulfilled. Moreover, it survives for rather larger frequencies that breaks the adiabatic condition, which is understood by considering the so-called dynamical localization. It implies that the periodic atom-molecule conversion is more robust than we expect from the semiclassical approximation. We also show that for much larger frequencies delocalization takes place so that the dynamics becomes diffusive.

DOI: [10.1103/PhysRevA.93.013616](https://doi.org/10.1103/PhysRevA.93.013616)**I. INTRODUCTION**

Feshbach resonance is an essential ingredient to control effective interaction between atoms by varying an external parameter such as magnetic field [1]. It appears when the energies of two incoming atoms match that of the molecular bound state formed by them. In magnetic Feshbach resonance, energy detuning between a bound molecule and atoms can be controlled via magnetic field since they have different magnetic moments [2,3]. As the detuning, the energy of the molecular bound state minus that of atoms, varies from large positive, where atoms dominate, to large negative values, atoms are transformed into molecules. One of the important issues is how a large fraction of atoms is smoothly transformed into molecules when the detuning varies slowly enough. It has been found that the conversion of atoms to molecules is not perfect during the adiabatic passage across the Feshbach resonance [4–11]. The amount of remaining atoms is not simply explained by the Landau-Zener formula, which leads us to take the many-body effect into account. Note that there has been special interest in the breakdown of adiabaticity in many-body systems [12,13]. The so-called spin-boson model [8–11,14] has been extensively investigated to understand nonadiabatic dynamics of the molecular production of many-body systems in the semiclassical limit.

So far the main interest has been in varying detuning linearly in time, called a linear sweep. However, there are several reasons to consider periodic sweepings. It has been theoretically proposed to measure the equilibrium gap of the fermionic superfluid using a sinusoidal modulation of *s*-wave scattering length [15]. Production of ultracold bosonic molecules with a periodic magnetic modulation has also been observed experimentally [16] and discussed theoretically [17,18]. Moreover, nonequilibrium quantum phase transitions were investigated in various systems by using a periodic sinusoidal modulation [19]. In Ref. [20] the exactly same Hamiltonian that we consider here was analytically studied in the context of the Bethe ansatz.

In this paper we investigate the atom-molecule conversion when the detuning varies periodically in time both

semiclassically and quantum mechanically. We have found four dynamically distinct regimes exist depending on the driving frequencies. Namely adiabatic, localized, diffusive, and high-frequency regimes sequentially appear as the driving frequency increases. In the adiabatic regime with tiny frequencies the regular periodic conversion between atoms and molecules are observed in quantum mechanics so that it can be regarded as the adiabatic regime, while extremely slow chaotic diffusion in the molecular fraction occurs in semiclassical dynamics due to the so-called separatrix crossing [21–25]. In the localized regime the periodic conversion continues to take place like the adiabatic regime in quantum mechanics due to the so-called dynamical localization [26–28], while the diffusion in the semiclassical limit occurs faster than the adiabatic case, so the regular atom-molecule conversion disappears relatively soon. In the diffusive regime, both semiclassical and quantum mechanics exhibit diffusive dynamics in the molecular fraction such that periodic conversion immediately dies. As the frequency becomes bigger and bigger, the system in the semiclassical limit evolves through complicated motions of the so-called mixed phase space, where regular and chaotic motions coexist, finally to predominantly regular motions.

This paper is organized as follows. In Sec. II we describe the model that we investigate, namely the periodically driven spin-boson model both semiclassically and quantum mechanically. In Sec. III we present the main results of this paper; the dynamics of the driven spin-boson model is categorized into four regimes, namely adiabatic, localized, diffusive, and high-frequency regimes. We also briefly discuss the possibility that our theoretical findings are experimentally justifiable. Finally we summarize our results in Sec. IV.

II. PERIODICALLY DRIVEN SPIN-BOSON MODEL

We introduce a Hamiltonian describing atom-molecule conversion across the Feshbach resonance [10,11],

$$\hat{H} = \frac{\delta(t)}{2} \hat{b}^\dagger \hat{b} - \frac{\delta(t)}{2} \frac{1}{2} \sum_{i=1}^N (\hat{a}_{i\uparrow}^\dagger \hat{a}_{i\uparrow} + \hat{a}_{i\downarrow}^\dagger \hat{a}_{i\downarrow}) + \frac{g}{\sqrt{N}} \sum_{i=1}^N (\hat{b} \hat{a}_{i\uparrow}^\dagger \hat{a}_{i\downarrow}^\dagger + \hat{b}^\dagger \hat{a}_{i\downarrow} \hat{a}_{i\uparrow}), \quad (1)$$

*swkim0412@pusan.ac.kr

where $\hat{a}_{i\sigma}$ with $\sigma = \uparrow, \downarrow$ and \hat{b} are annihilation operators of a fermionic atom and a bosonic molecule, respectively. They satisfy the conservation relation $\sum_{i\sigma} \hat{a}_{i\sigma}^\dagger \hat{a}_{i\sigma} + 2\hat{b}^\dagger \hat{b} = 2N$. The first and the second term of the Hamiltonian (1) represent the ground-state energy of the bosonic molecules and the fermionic atoms, respectively. $\delta(t)$ and g denote a (time-dependent) detuning and a coupling strength, respectively. The signs of the first and the second term of (1) are opposite so that when $|\delta(t)|$ is large enough, the system prefers to be $2N$ fermions as a ground state for $\delta(t) > 0$ while N bosonic molecules for $\delta(t) < 0$. In order to describe the conversion from atoms to molecules and vice versa, $\delta(t)$ should vary from large positive to negative values. The third term describes the conversion process between the atoms and the molecules.

By using the so-called Anderson pseudospin operators, $\hat{S}_+ = \sum_{i=1}^N \hat{a}_{i\uparrow}^\dagger \hat{a}_{i\downarrow}$, $\hat{S}_- = \hat{S}_+^\dagger$, and $\hat{S}_z = (1/2) \sum_{i=1}^N (\hat{f}_{i\uparrow} + \hat{f}_{i\downarrow} - 1)$ with $\hat{f}_{i\sigma} = \hat{a}_{i\sigma}^\dagger \hat{a}_{i\sigma}$ ($\sigma = \uparrow, \downarrow$), the Hamiltonian (1) is rewritten as a more compact form [9,10,29],

$$\hat{H}_{\text{SB}} = \delta(t) \hat{b}^\dagger \hat{b} + \frac{g}{\sqrt{N}} (\hat{b}^\dagger \hat{S}_- + \hat{b} \hat{S}_+). \quad (2)$$

This is called as spin-boson model. The bases of Hamiltonian (2) are chosen as $|n_b\rangle_b |S_z\rangle_S$, where the former and the latter represent the bosonic state with its number n_b and the spin state with z -component S_z , respectively. The conservation relation is now expressed as $\hat{b}^\dagger \hat{b} + \hat{S}_z = N/2$ so that the bases are labeled simply by n_b according to $|n_b\rangle = |n_b\rangle_b |N/2 - n_b\rangle_S$. For convenience we scale energies and time with g : $\hat{H}_{\text{SB}}/g \rightarrow \hat{H}_{\text{SB}}$, $gt \rightarrow t$, and $\delta/g \rightarrow \delta$.

In the semiclassical limit $N \gg 1$, the quantum mechanical operators can be replaced by the corresponding complex numbers, e.g., $\hat{b} \rightarrow b = e^{-i\varphi} \sqrt{n_b}$ and $\hat{S}_+ \rightarrow S_+ = S \sin \theta e^{i\xi}$. By considering the number conservation relation,

$$n_b + (N/2) \cos \theta = N/2, \quad (3)$$

the semiclassical Hamiltonian is obtained as

$$H_{\text{SB}} = \delta(t) n_b - 2n_b \sqrt{1 - \frac{n_b}{N}} \cos \phi, \quad (4)$$

with $\phi = \varphi - \xi - \pi$ ($-\pi \leq \phi \leq \pi$). With scaling $n_b/N = n$ ($0 \leq n \leq 1$) and $H_{\text{SB}}/N = h_{\text{SB}}$, we end up with the Hamiltonian,

$$h_{\text{SB}} = \delta(t) n - 2n \sqrt{1 - n} \cos \phi. \quad (5)$$

Here n and ϕ satisfy $\{\phi, n\} = 1$, where $\{\}$ denotes the Poisson bracket. In the limit $|\delta(t)| \gg 1$, the Hamiltonian (5) is approximated to $h_{\text{SB}} \simeq \delta(t) n$. Thus ϕ becomes cyclic so that n is conserved since the equations of motion are $\dot{n} = -\partial_\phi h_{\text{SB}} \simeq 0$ and $\dot{\phi} = \partial_n h_{\text{SB}} \simeq \delta_1$.

In this paper we consider a sinusoidal modulation of the detuning:

$$\delta(t) = \delta_1 \cos(\omega t + \phi_d). \quad (6)$$

Note that δ_1 and ω are also scaled as $\delta_1/g \rightarrow \delta_1$ and $\omega/g \rightarrow \omega$. In order to focus on how the dynamics depends on ω , we set $\delta_1 = 10$ and $\phi_d = 0$ such that $\delta(t=0) = \delta_1$, which implies the initial ground state of (2) is atom-dominated, namely $n_b \sim 0$.

To compare quantum analysis with the semiclassical one on the equal footing, we need the corresponding semiclassical

distribution of the initial quantum state, namely the ground state of \hat{H}_{SB} at $t = 0$. We use the Husimi distribution function, which can be obtained from smoothing the Wigner function with coherent states [30]. Here we exploit the coherent spin state [31] defined as [32]

$$|\theta, \phi\rangle = \sum_{m=0}^N \sqrt{\frac{N!}{m!(N-m)!}} \cos^{N-m} \left(\frac{\theta}{2} \right) \sin^m \left(\frac{\theta}{2} \right) \times e^{-i(2m-N)(\phi+\pi)/2} |m\rangle. \quad (7)$$

By using $\sin(\theta/2) = \sqrt{n}$ and $\cos(\theta/2) = \sqrt{1-n}$ derived from Eq. (3), the coherent spin state is rewritten as

$$|n, \phi\rangle = \sum_{m=0}^N \sqrt{\frac{N!}{m!(N-m)!}} (1-n)^{\frac{N-m}{2}} n^{\frac{m}{2}} \times e^{-i(2m-N)(\phi+\pi)/2} |m\rangle. \quad (8)$$

Then the Husimi distribution function is $|\langle n, \phi | \psi \rangle|^2$ for a quantum state $|\psi\rangle$. In this paper the initial state is chosen as the ground state of \hat{H}_{SB} at $t = 0$, which is nearly close to $|n=0\rangle$. It means that the system is prepared with only fermionic atoms rather than molecules in quantum mechanics. The corresponding semiclassical density in phase space is described by the Husimi distribution function for the ground state, as shown in Fig. 6(a).

The quantum dynamics is numerically calculated by solving the time-dependent Schrödinger equation. We calculate the semiclassical dynamics using equations of motion in Appendix. These calculations are performed based on the fourth-order Runge-Kutta method.

III. RESULTS

A. Adiabatic regime

First, let us consider the adiabatic regime. It is nontrivial to define the criterion of the adiabatic condition for a given quantum dynamics [33]. We numerically found that when $\omega \ll 1/(N\delta_1)$, the quantum dynamics is adiabatic in which the system follows the ground state of the Hamiltonian (2). Atoms are converted to molecules periodically and vice versa without any noticeable decay. Thus, the frequency $\Omega_a = 1/(N\delta_1)$ provides the border between the adiabatic and localized regime. Here we use $N = 80$ and $\delta_1 = 10$, so $\Omega_a = 1.25 \times 10^{-3}$. We note that the border Ω_a is still less than the frequency obtained by the well-known adiabatic condition,

$$\omega \ll \frac{(E_1(u) - E_0(u))^2}{|\langle \varphi_1(u) | \frac{\partial \hat{H}_{\text{SB}}}{\partial u} | \varphi_0(u) \rangle|}, \quad (9)$$

where $\{E_k(u)\}$ and $\{|\varphi_k(u)\rangle\}$ are the instantaneous eigenvalues and eigenstates of $\hat{H}_{\text{SB}}(u)$ at $u = \omega t$, respectively [34,35]. Using the same N and δ_1 , the right side of (9) is close to 7×10^{-3} , which is about five times larger than Ω_a . Thus the criterion $\omega \ll \Omega_a = 1/(N\delta_1)$ already satisfies the quantum adiabatic condition.

Figure 1 presents $\langle n \rangle$ ($\langle \cdot \rangle$ denotes quantum mechanical average) of the quantum dynamics of the spin-boson model as function of t/T , where T represents the period of the driving $T = 2\pi/\omega$, with $\omega = 1.25 \times 10^{-4}$ ($=0.1\Omega_a$) implying

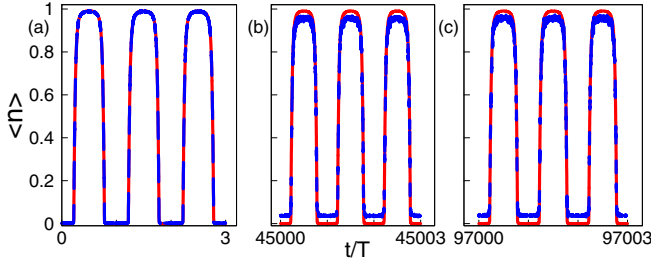


FIG. 1. Evolution of $\langle n \rangle$ with $\omega = 1.25 \times 10^{-4} (= \Omega_a/10)$ for the quantum (solid red line) and the semiclassical (blue dashed line) dynamics for (a) $0 \leq t/T \leq 3$, (b) $45000 \leq t/T \leq 45003$, (c) $97000 \leq t/T \leq 97003$.

it satisfies the adiabatic condition. This clearly shows the atom-molecule conversion periodically occurs for a considerably long time scale. However, the corresponding semiclassical dynamics behaves quite differently; it exhibits damped oscillation approaching $n = 0.5$, similar to Figs. 3(a)–3(c), *extremely slowly* (not shown) due to the so-called separatrix crossing [21–25].

A typical Hamiltonian to describe the separatrix crossing is

$$H(t) = \frac{J^2}{2} + A \sin \omega t \cos \phi. \quad (10)$$

Without time dependence this corresponds to a trivial pendulum Hamiltonian [36]. Usually Hamiltonian chaos has been studied in the mechanical pendulum perturbed by an additional time-dependent term, i.e., $J^2/2 + A \sin \phi + B \phi \cos \omega t$. As B increases, chaotic motion forms near separatrices. Note that the chaotic region is localized near the separatrices unless B is not large enough. In Eq. (10), however, the size of the separatrices themselves oscillate in time according to $A \sin \omega t$. As far as the Liouville theorem, requiring that the area in phase space should be conserved, is concerned, phase points enclosed by the separatrices should cross them so as to form homoclonic tangles, a signature of chaos. Therefore, the area enclosed by the separatrix of the Hamiltonian (10) becomes chaotic no matter how small ω is.

The phase space portraits of Hamiltonian (5) are presented in Fig. 2 at several δ 's [11,14,37,38]. It clearly shows that a separatrix forms around $n = 0$ and grows to cover the whole n , $[0, 1]$, as δ goes from $\delta = 2$ to 0. Then it decreases and shrinks to disappear as δ goes from $\delta = 0$ to -2 . As δ varies from $\delta = 2$ to $\delta = -2$, the separatrix sweeps the whole phase space so that the semiclassical dynamics becomes fully chaotic no matter how small ω is. Thus when the detuning slowly changes periodically as $\delta = \delta_1 \cos(\omega t)$ with a large δ_1 , the semiclassical dynamics is always diffusive or chaotic. The oscillation of the atom-molecule conversion gradually vanishes and it saturates to $n = 0.5$. In this regime, however, we find that the quantum dynamics exhibits adiabatic behavior, i.e., the regular oscillation of n or periodic atom-molecule conversion when δ varies slowly satisfying $\omega \ll \Omega_a$.

A remark is in order. The inevitable breakdown of the adiabatic condition for the slow dynamics in many-body systems has been an issue [12,13]. It has been confirmed using the spin-boson Hamiltonian (2) with semiclassical approximation [10]. Interestingly the adiabatic behavior survives if the

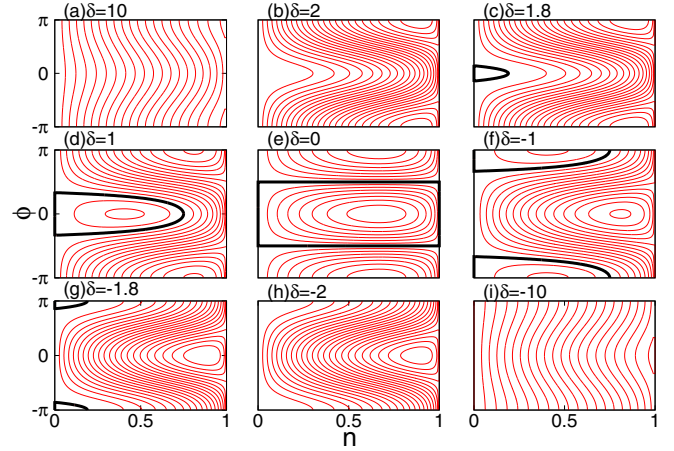


FIG. 2. Phase space portraits of the Hamiltonian (5) for several δ with $\omega = 0$, where we ignore time dependence. The thick black curves represent the separatrices.

spin-boson model is quantum mechanically treated, implying that experiments done with rather smaller particles (not in the semiclassical regime) may exhibit adiabatic behavior rather than its breakdown.

B. Localized regime

For $\omega \gtrsim \Omega_a (= 1.25 \times 10^{-3})$ the quantum state deviates from the instantaneous ground state of the Hamiltonian (2), and the quantum dynamics becomes nonadiabatic. One thus expects the atom-molecule conversion no longer periodically occurs. However, Figs. 3(a)–3(c) shows $\langle n \rangle$ of quantum mechanics with $\omega = 1.25 \times 10^{-2} (= 10\Omega_a)$ still exhibits a pretty good periodic oscillation although it is not perfect compared with the adiabatic case, while the oscillation rather quickly dies in the semiclassical approximation. The survival of the

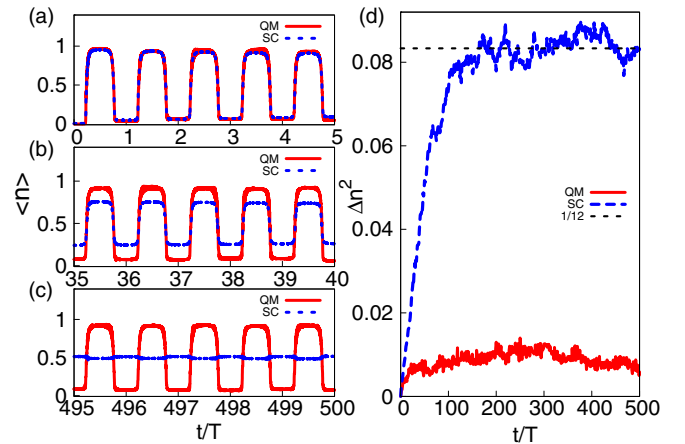


FIG. 3. Evolution of $\langle n \rangle$ in the quantum (red solid lines) and semiclassical limit (blue dashed lines) with $\omega = 1.25 \times 10^{-2} (= 10\Omega_a)$ for (a) $0 \leq t/T \leq 5$, (b) $35 \leq t/T \leq 40$, and (c) $495 \leq t/T \leq 500$. (d) The evolution of the variance Δn^2 for the quantum (red solid line) and the semiclassical case (blue dashed line) at multiples of the period. The dotted horizontal line $\Delta n^2 \sim 0.083$ ($\sim 1/12$) represents the classical ergodic limit.

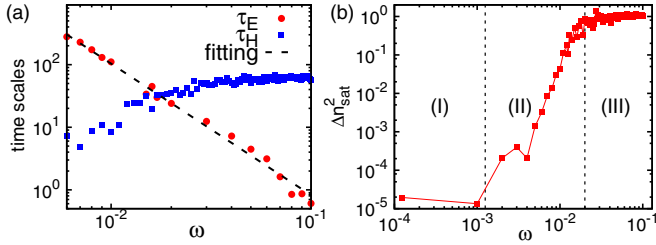


FIG. 4. Log-log plot for the time scales and the variance as a function of ω . (a) τ_E (red circle dots) and τ_H (blue square dots). The dashed black line is the fitting curve of τ_E , which is given by $\tau_E \sim \omega^{-2.1}$. (b) Quantum variances at saturation. It is normalized by the classical ergodic limit. Three distinct regimes are visible: (I) adiabatic ($\omega \ll \Omega_a$), (II) localized ($\Omega_a \lesssim \omega \lesssim \Omega_l$), and (III) diffusive regime ($\omega \gtrsim \Omega_l$).

oscillation in quantum mechanics in the nonadiabatic regime can be understood by considering the so-called dynamical localization [26–28].

A fully chaotic system in classical mechanics exhibits diffusive behavior so that it spontaneously evolves to the so-called ergodic state [26,39–41], where the whole available phase space is uniformly covered whatever initial distribution it starts from. This is nothing but relaxation to equilibrium. There is a time scale t_E , called the ergodic time [26,39,41], on how long it takes to reach the ergodic state. In quantum mechanics, another new time scale, the so-called Heisenberg time t_H [26,39–41] defined as $1/\Delta\varepsilon$, where $\Delta\varepsilon$ denotes the mean level spacing of the quasienergy, comes into play. Roughly speaking, when the Heisenberg time is reached, the system starts to see the discreteness of energy levels due to Heisenberg’s uncertain principle so that the chaotic diffusion stops. If $t_H < t_E$, the diffusion stops in quantum mechanics while it continues in the corresponding classical mechanics. Such quantum prohibition of diffusion gives rise to the localization, which is the dynamical localization. It is well known that the dynamical localization of the quantum kicked rotor is mathematically equivalent to the Anderson localization of disordered lattices [26,39–41].

We emphasize that the dynamical localization in this paper is considered only at multiples of the period, $t = kT, k = 0, 1, \dots$ [42]. Figure 3(d) shows the variance of n , Δn^2 defined as $\langle n^2 \rangle - \langle n \rangle^2$, as a function of k both in the quantum and in the semiclassical case at $\omega = 10\Omega_a$. The semiclassical variance is saturated around $\tau_E = t_E/T$, while the quantum variance stops increasing around $\tau_H = t_H/T (< \tau_E)$ where the quantum localization takes place. In the semiclassical case, for the whole available phase space $0 \leq \phi < 2\pi$ and $0 \leq n < 1$, $\langle \Delta n^2 \rangle$ is given as $1/12$ if the state is fully ergodic, or uniformly distributed over the whole phase space. The bigger ω the faster the chaotic diffusion. Thus, the ergodic time decreases when ω increases as $\tau_E \sim \omega^{-2.1}$ [Fig. 4(a)]. However, the Heisenberg time τ_H increases as ω increases as shown in Fig. 4(a), which is discussed in the next paragraph. It causes the transition from $\tau_H < \tau_E$ to $\tau_H > \tau_E$, i.e., from localization to delocalization, to occur around $\omega \sim 0.02$ as shown in Fig. 4(b). It gives the border between the localized and the diffusive regime, denoted as $\Omega_l (\sim 0.02)$.

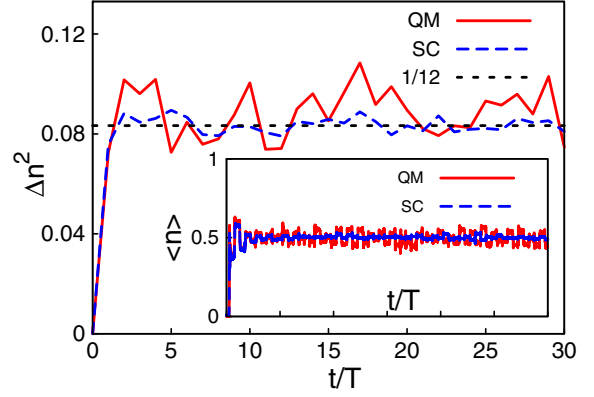


FIG. 5. Evolution of the variance $\langle \Delta n^2 \rangle$ for the quantum (the red solid curve) and the semiclassical case (the blue dashed curve) with $\omega = 0.125$ at multiples of the time period. The dotted horizontal line $\langle \Delta n^2 \rangle \sim 1/12$ represents the classical ergodic limit. The inset presents the evolution of $\langle n \rangle$ for $0 \leq t/T \leq 30$.

Now we qualitatively explain why τ_H increases as ω increases. Since the Hamiltonian considered here is time periodic, i.e., $\hat{H}_{SB}(t) = \hat{H}_{SB}(t + T)$, according to the so-called Floquet theory [40,41] any state can be expanded as

$$|\psi(kT)\rangle = \sum_{\alpha} \exp(-i\varepsilon_{\alpha}kT) \langle v_{\alpha} | \psi(0) \rangle |v_{\alpha}\rangle. \quad (11)$$

Here the quasienergy ε_{α} ($0 \leq \varepsilon_{\alpha} < \omega$) and the Floquet state $|v_{\alpha}\rangle$ satisfy

$$\hat{U} |v_{\alpha}\rangle = e^{-i\varepsilon_{\alpha}T} |v_{\alpha}\rangle, \quad (12)$$

with a unitary operator $\hat{U} = \hat{T} e^{-i \int_0^T \hat{H}_{SB}(t) dt}$, where \hat{T} represents the operator of time ordering. The mean level spacing of quasienergies $\Delta\varepsilon$ is not straightforwardly defined so we can roughly define it as ω/N_c , where N_c denotes the number of the operational Floquet states covering the initial state. More precisely $\sum_{\alpha=1}^{N_c-1} |\langle v_{\alpha} | \psi(0) \rangle|^2 \leq r$ and $\sum_{\alpha=1}^{N_c} |\langle v_{\alpha} | \psi(0) \rangle|^2 > r$, where $|\langle v_{\alpha} | \psi(0) \rangle|^2$ are arranged in descending order. Here we set $r = 0.99$ [41,43,44]. We then find the Heisenberg time $t_H/T \sim 2\pi / (\langle \Delta\varepsilon \rangle T) \sim N_c$. In the adiabatic limit we have $N_c \sim 1$ since the dynamics is governed by a single state. We expect N_c might increase as ω increases since the bigger ω the more interlevel transition occurs in the sense of the Landau-Zener transition.

C. Diffusive regime

Figure 5 shows that both the quantum and classical variance quickly approach the classical ergodic limit. $\langle n \rangle$ is also relaxed and it does not exhibit periodic atom-molecule conversion with $\omega = 0.125 (> \Omega_l)$. The Husimi plot of the quantum state exhibits complicated mixtures of atoms and molecule as shown in Fig. 6(d). For comparison we also present the Husimi plot for the localized regime in Fig. 6(c).

Figure 4(b) shows the saturated value of the quantum variance $\langle \Delta n^2 \rangle$ [44]. It is normalized by the classical ergodic limit, namely $1/12$. Here the transition from the localized to the delocalized regime is clearly visible around $\Omega_l (\sim 0.02)$. Note that the adiabatic border lies at $\Omega_a = 1.25 \times 10^{-3}$. The periodic atom-molecule conversion of the spin-boson model

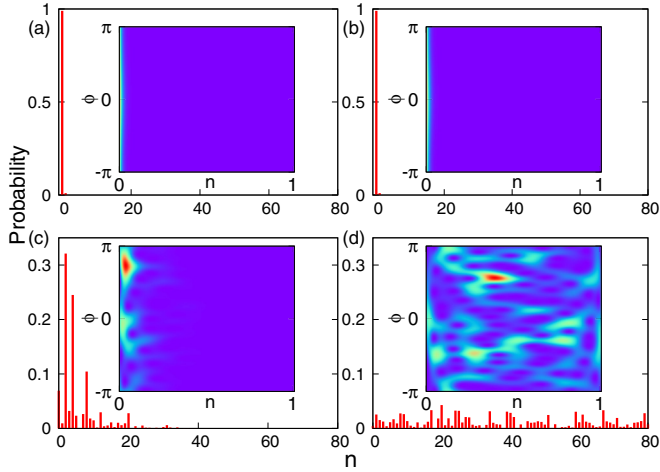


FIG. 6. Probability distributions of the quantum states: (a) initial state, (b) adiabatic regime, (c) of the localized regime ($\omega = 1.25 \times 10^{-2}$) at $t = 500T$, and (d) of the diffusive regime ($\omega = 1.25 \times 10^{-1}$) $t = 15T$, at which the variances are saturated to the classical ergodic limit. The insets show the corresponding Husimi plots.

survives for $\Omega_a \lesssim \omega \lesssim \Omega_l$, which is unexpected from considering only the adiabatic condition. For $\Omega_l \lesssim \omega$ the variance reaches the classical limit implying dynamical localization no longer occurs. Even in quantum mechanics the dynamics is then predominantly chaotic or diffusive so that reliable atom-molecule conversion no longer exists.

D. High-frequency regime

Roughly speaking the energy difference between the atoms and the molecules is given as δ_1 at $\omega = 0$ and it is the highest natural frequency of the nondriven case. If ω is larger than or equal to δ_1 , the direct quantum transition between atoms and molecules can take place. It leads to make the conversion dynamics more complex. Thus for $\omega \gtrsim \delta_1$ the periodic conversion with frequency ω cannot be guaranteed. It is known that the dynamics of a system for the high-frequency regime can be described by effective time-independent Hamiltonians [45–49]. In this paper we are interested in controllable atom-molecule conversion using periodic driving. Thus we limit our consideration to $\omega \ll \delta_1 (=10)$. For completeness, however, we briefly summarize the dynamics of the atom-molecule conversion below.

Beyond the diffusive regime, $\omega > \Omega_d (\sim 1.07)$, the quantum $\langle n \rangle$ starts to oscillate again even though the corresponding semiclassical $\langle n \rangle$ does not as shown in Fig. 7(a). In this case the dynamics undergoes transition from complete chaos of the diffusive regime to dynamics with mixed phase space as shown in the inset of Fig. 7(a). For much higher ω , namely ~ 10 , the dynamics eventually becomes regular. For intermediate frequencies the evolutions of $\langle n \rangle$ exhibits various behaviors as shown in Figs. 7(b) and 7(c). If a stability island appears near $n \sim 0$ as shown in the inset of Fig. 7(b), $\langle n \rangle$ stays at 0. This is similar to the so-called self-trapping of two weakly coupled Bose-Einstein condensates driven by periodic modulation [50]. In Fig. 7(c) $\langle n \rangle$ slowly oscillates both in the quantum and semiclassical cases. The behaviors observed

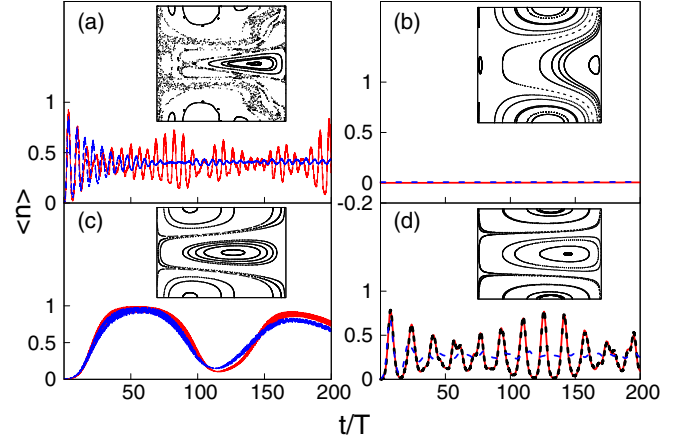


FIG. 7. Evolution of $\langle n \rangle$ for the quantum (the red solid curves) and semiclassical dynamics (the blue dashed curves) with (a) $\omega = 1.32$, (b) $\omega = 4.05$, (c) $\omega = 4.40$, and (d) $\omega = \delta_1 = 10$. The x axis is the time divided by the period T . The black long dashed curve in (d) is calculated by using the Hamiltonian (13). The insets show the corresponding classical Poincaré surface of sections. Here the x axis is n and the y axis is ϕ .

here depend on the characteristics of the motions near $n \sim 0$ of phase space at which the initial condition is posed.

It has been shown that for $\omega \gg 1$, the Hamiltonian (2) can be approximated to the following form [51–53]:

$$\hat{H}_{SB}^R = \frac{J_0(\delta_1/\omega)}{\sqrt{N}} (\hat{b} \hat{S}_+ + \hat{b}^\dagger \hat{S}_-), \quad (13)$$

where $J_0(\cdot)$ is the zeroth order of the Bessel function. This effective Hamiltonian well describes the quantum dynamics in the high-frequency regime as shown in Fig. 7(d).

E. Discussion

Here we discuss the possibility that our theoretical finding is experimentally justifiable. Through this paper we assume single-mode, zero-temperature, and uniform condensate for our system. However, long-lasting strong external driving may induce heating to make the above mentioned assumptions broken. To determine whether such heating influences our results we need to know several important time scales. Unfortunately, it is not easy to accurately estimate them since we consider a somewhat unusual situation with a rather small number of particles, namely 80 bosonic (fermionic) molecules (atomic pairs). Compared with 10^5 to 10^7 atoms in typical experiments [6,54,55], a small number of particles with $N = 80$ was considered in this paper. The reason is that our main concern lies at observing the quantum effect which vanishes in the semiclassical limit, $N \rightarrow \infty$.

We assume that the mean density $n_d = 10^{18} \text{ m}^{-3}$, geometric frequency of a harmonic trap $\bar{\omega} = 3.14 \text{ kHz}$, and temperature of fermions $\Theta/\Theta_F = 0.05$, where the Fermi temperature is denoted as $\Theta_F = 187 \text{ nK}$ [2]. The border between the adiabatic and localized regime is given as $T_a = 0.7 \text{ ms}$ with $2\pi/\Omega_a$. Here we have $\Omega_a = 1.25 \times 10^{-3} g \sqrt{n_d}/\hbar$ without scaling and the coupling strength $g = \sqrt{4\pi \hbar^2 a_{bg} \Delta \mu \Delta B/m_l}$, where we use $a_{bg} = 1405 a_0$ with the Bohr radius a_0 , $\Delta \mu = 2\mu_B$ with the Bohr magneton μ_B , $\Delta B = 300 \text{ G}$, and the mass of ${}^6\text{Li}$. We also

find the relaxation time $T_R \simeq \hbar E_F / (k_B \Theta)^2 \sim 16$ ms [55,56] and the period of harmonic motion in the trap $T_l \sim 2$ ms.

For the adiabatic regime shown in Fig. 1, where we have $T = 10T_a = 7$ ms, it is unlikely to observe the oscillation of $\langle n \rangle$ for quite a long time, namely $100\,000T$. Only after two periods (~ 14 ms), the heating becomes considerable due to relaxation with $T_R \sim 16$ ms. Moreover the motion itself of the particles in the trap cannot be ignored due to $T > T_l$. For the localized regime shown in Fig. 3, where we have $T = 0.1T_a \sim 0.07$ ms $\ll T_R$ and $T_l/T \sim 28$, one might observe the coherent oscillation of $\langle n \rangle$ supported by the dynamical localization. Note that the oscillation should be maintained for $20 \sim 30$ periods in order to observe the localization. However it is not completely clear whether such direct substitution of $N = 80$, which is extremely small, into the formula developed in the typical experimental condition with large N [1,2]. Even if all the above conditions are satisfied, the nonuniformity still makes additional problems. For example, assumptions of the single mode is guaranteed when $g\sqrt{n} \gg k_B \Theta$ [17,57] is satisfied. Since the density is low near the tail of the trap, atomic clouds near the surface of the trap might violate the single-mode assumption.

IV. SUMMARY

We have studied the dynamics of the atom-molecule conversion using the spin-boson model driven periodically. We have found four distinct regimes as the driving frequency increases; adiabatic, localized, diffusive, and high-frequency regimes. In the adiabatic regime, the regular periodic conversion occurs in quantum dynamics while slow chaotic diffusion due to separatrix crossing takes place in the semiclassical one. In the localized regime the regular conversion still survives in quantum dynamics even if the quantum adiabatic condition is broken. This is explained by the dynamical localization. Therefore, we can say that the periodic atom-molecule conversion is more robust than one expects from semiclassical consideration. Once the dynamical localization no longer works, the chaotic diffusion occurs even in quantum dynamics so as for the periodic conversion to die. This is the diffusive regime. For higher frequencies the semiclassical dynamics finally becomes regular via complicated dynamics with mixed phase space.

ACKNOWLEDGMENTS

This work was supported by a two-year research grant of Pusan National University.

APPENDIX: EQUATIONS OF MOTION IN THE SEMICLASSICAL LIMIT

We derive the Hamiltonian equations of motion for the semiclassical dynamics [14]. We introduce Q and P satisfying

$$b = \frac{1}{\sqrt{2}}(Q + iP), \quad (\text{A1})$$

with $\{Q, P\} = 1$. We normalize Q , P , and spins using N :

$$Q = \sqrt{N}q, \quad P = \sqrt{N}p, \quad S_i = \frac{N}{2}s_i, \quad (i = x, y, z). \quad (\text{A2})$$

Then the semiclassical Hamiltonian h_{SB} is rewritten as

$$h_{\text{SB}} = \frac{\delta}{2}(q^2 + p^2) + \frac{1}{2\sqrt{2}N}((q - ip)s_- + (q + ip)s_+). \quad (\text{A3})$$

Poisson bracket relations are modified as the following:

$$\begin{aligned} \{q, p\} &= \frac{1}{N}, & \{s_x, s_{\pm}\} &= \pm \frac{2i}{N}s_z, \\ \{s_y, s_{\pm}\} &= -\frac{2}{N}s_z, & \{s_z, s_{\pm}\} &= \mp \frac{2i}{N}s_{\pm}. \end{aligned} \quad (\text{A4})$$

The equations of motion for the Hamiltonian (A3) are

$$\frac{dq}{dt} = N\{q, h_{\text{SB}}\} = \delta p - \frac{s_y}{\sqrt{2}}, \quad (\text{A5})$$

$$\frac{dp}{dt} = N\{p, h_{\text{SB}}\} = -\delta q - \frac{s_x}{\sqrt{2}}, \quad (\text{A6})$$

$$\frac{ds_x}{dt} = N\{s_x, h_{\text{SB}}\} = -\sqrt{2}ps_z, \quad (\text{A7})$$

$$\frac{ds_y}{dt} = N\{s_y, h_{\text{SB}}\} = -\sqrt{2}qs_z, \quad (\text{A8})$$

$$\frac{ds_z}{dt} = N\{s_z, h_{\text{SB}}\} = \sqrt{2}(qs_y + ps_x). \quad (\text{A9})$$

These equations are exploited for the numerical calculation of the semiclassical dynamics. The molecular fraction n and ϕ are obtained by $n = \frac{1}{2}(1 - s_z)$ and $\phi = \text{Arg}[(q - ip)(s_x - is_y)] - \pi$.

-
- [1] C. J. Pethick and H. Smith, in *Bose-Einstein Condensation*, 2nd ed. (Cambridge University Press, New York, 2008), Chap. 5.
- [2] W. Ketterle and M. W. Zwierlein, in *Ultracold Fermi Gases, Proceedings of International School of Physics "Enrico Fermi,"* edited by M. Inguscio, W. Ketterle, and C. Salomon (IOS Press, Amsterdam, 2008), Course CLXIV.
- [3] C. Chin, R. Grimm, P. Julienne, and E. Tiesinga, *Rev. Mod. Phys.* **82**, 1225 (2010).
- [4] C. A. Regal, C. Ticknor, J. L. Bohn, and D. S. Jin, *Nature (London)* **424**, 47 (2003).
- [5] K. E. Strecker, G. B. Partridge, and R. G. Hulet, *Phys. Rev. Lett.* **91**, 080406 (2003).
- [6] J. Cubizolles, T. Bourdel, S. J. J. M. F. Kokkelmans, G. V. Shlyapnikov, and C. Salomon, *Phys. Rev. Lett.* **91**, 240401 (2003).
- [7] E. Hodby, S. T. Thompson, C. A. Regal, M. Greiner, A. C. Wilson, D. S. Jin, E. A. Cornell, and C. E. Wieman, *Phys. Rev. Lett.* **94**, 120402 (2005).
- [8] I. Tikhonenkov, E. Pazy, Y. B. Band, M. Fleischhauer, and A. Vardi, *Phys. Rev. A* **73**, 043605 (2006).

- [9] D. Sun, A. Abanov, and V. Pokrovsky, *EPL* **83**, 16003 (2008).
- [10] A. Altland, V. Gurarie, T. Kriecherbauer, and A. Polkovnikov, *Phys. Rev. A* **79**, 042703 (2009).
- [11] A. P. Itin and P. Törmä, *Phys. Rev. A* **79**, 055602 (2009).
- [12] A. Polkovnikov and V. Gritsev, *Nat. Phys.* **4**, 477 (2008).
- [13] A. Polkovnikov, K. Sengupta, A. Silva, and M. Vengalattore, *Rev. Mod. Phys.* **83**, 863 (2011).
- [14] A. P. Itin and P. Törmä, [arXiv:0901.4778](https://arxiv.org/abs/0901.4778).
- [15] R. G. Scott, F. Dalfovo, L. P. Pitaevskii, and S. Stringari, *Phys. Rev. A* **86**, 053604 (2012).
- [16] S. T. Thompson, E. Hodby, and C. E. Wieman, *Phys. Rev. Lett.* **95**, 190404 (2005).
- [17] B. Liu, L.-B. Fu, and J. Liu, *Phys. Rev. A* **81**, 013602 (2010).
- [18] V. M. Bastidas, C. Emary, B. Regler, and T. Brandes, *Phys. Rev. Lett.* **108**, 043003 (2012).
- [19] S.-C. Li and L.-C. Zhao, *J. Opt. Soc. Am. B* **31**, 642 (2014).
- [20] P. Barmettler, D. Fioretto, and V. Gritsev, *EPL (Europhys. Lett.)* **104**, 10004 (2013).
- [21] A. I. Neishtadt, *Sov. J. Plasma Phys.* **12**, 568 (1986).
- [22] J. R. Cary, D. F. Escande, and J. L. Tennyson, *Phys. Rev. A* **34**, 4256 (1986).
- [23] D. Bruhwiler and J. R. Cary, *Physica D* **40**, 265 (1989).
- [24] V. I. Arnold, V. V. Kozlov, and A. I. Neishtadt, *Mathematical Aspect of Classical and Celestial Mechanics*, 3rd ed. (Springer-Verlag, New York, 2006).
- [25] A. J. Lichtenberg and M. A. Leiberman, *Regular and Chaotic Dynamics*, 2nd ed. (Springer-Verlag, New York, 1992).
- [26] G. Casati and B. Chirikov (eds.), in *Quantum Chaos: Between Order and Disorder* (Cambridge University Press, Cambridge, 1995), pp. 1–38.
- [27] D. L. Shepelyansky, *Phys. Rev. Lett.* **56**, 677 (1986).
- [28] D. L. Shepelyansky, *Physica D* **28**, 103 (1987).
- [29] V. Gurarie, *Phys. Rev. A* **80**, 023626 (2009).
- [30] K. Takahashi and N. Saitōn, *Phys. Rev. Lett.* **55**, 645 (1985).
- [31] F. Trimborn, D. Witthaut, and H. J. Korsch, *Phys. Rev. A* **79**, 013608 (2009).
- [32] F. T. Arecchi, E. Courtens, R. Gilmore, and H. Thomas, *Phys. Rev. A* **6**, 2211 (1972).
- [33] D. Comparat, *Phys. Rev. A* **80**, 012106 (2009).
- [34] A. Messiah, *Quantum Mechanics*, Vol. 2 (North Holland, Amsterdam, 1962).
- [35] D. J. Griffiths, *Introduction To Quantum Mechanics*, 2/E (Pearson Education India, Delhi, 2005).
- [36] B. Mirbach and G. Casati, *Phys. Rev. Lett.* **83**, 1327 (1999).
- [37] A. Itin, A. Vasiliev, G. Krishna, and S. Watanabe, *Physica D* **232**, 108 (2007).
- [38] A. P. Itin and S. Watanabe, *Phys. Rev. E* **76**, 026218 (2007).
- [39] G. Casati, I. Guarneri, and U. Smilansky, *Quantum Chaos, Proceedings of the International School of Physics “Enrico Fermi”, Course CXIX, Varenna, 1991* (North-Holland, Amsterdam, 1993).
- [40] L. E. Reichl, *The Transition to Chaos*, 2nd ed. (Springer-Verlag, New York, 2003).
- [41] F. Haake, *Quantum Signatures of Chaos*, Vol. 54 (Springer, New York, 2010).
- [42] M. Grifoni and P. Hänggi, *Phys. Rep.* **304**, 229 (1998).
- [43] F. Haake, M. Kuś, and R. Scharf, *Zeitschrift für Physik B Condensed Matter* **65**, 381 (1987).
- [44] M. Machida, K. Saito, and S. Miyashita, *J. Phys. Soc. Jpn.* **71**, 2427 (2002).
- [45] M. Bukov, L. D’Alessio, and A. Polkovnikov, *Adv. Phys.* **64**, 139 (2015).
- [46] A. Eckardt and E. Anisimovas, *New J. Phys.* **17**, 093039 (2015).
- [47] A. P. Itin and M. I. Katsnelson, *Phys. Rev. Lett.* **115**, 075301 (2015).
- [48] A. Itin and A. Neishtadt, *Phys. Lett. A* **378**, 822 (2014).
- [49] S. Rahav, I. Gilary, and S. Fishman, *Phys. Rev. A* **68**, 013820 (2003).
- [50] G.-F. Wang, L.-B. Fu, and J. Liu, *Phys. Rev. A* **73**, 013619 (2006).
- [51] G. S. Agarwal and W. Harshawardhan, *Phys. Rev. A* **50**, R4465 (1994).
- [52] B. M. Garraway and N. V. Vitanov, *Phys. Rev. A* **55**, 4418 (1997).
- [53] S. Ashhab, J. R. Johansson, A. M. Zagoskin, and F. Nori, *Phys. Rev. A* **75**, 063414 (2007).
- [54] M. W. Zwierlein, C. A. Stan, C. H. Schunck, S. M. F. Raupach, A. J. Kerman, and W. Ketterle, *Phys. Rev. Lett.* **92**, 120403 (2004).
- [55] M. W. Zwierlein, C. H. Schunck, C. A. Stan, S. M. F. Raupach, and W. Ketterle, *Phys. Rev. Lett.* **94**, 180401 (2005).
- [56] L. D. Carr, G. V. Shlyapnikov, and Y. Castin, *Phys. Rev. Lett.* **92**, 150404 (2004).
- [57] J. Liu, B. Liu, and L.-B. Fu, *Phys. Rev. A* **78**, 013618 (2008).